

Measurement of open charm production in $d+Au$ collisions at $\sqrt{s_{NN}}=200$ GeV

An Tai† , for STAR Collaboration

Dept. of Physics, University of California at Los Angeles, Los Angeles, CA 90095

Abstract. We present the first comprehensive measurement of D^0, D^+, D^{*+} and their charge conjugate states at mid-rapidity in $d+Au$ collisions at $\sqrt{s_{NN}}=200$ GeV using the STAR TPC. The directly measured open charm multiplicity distribution covers a broad transverse momentum region of $0 < p_T < 11$ GeV/ c . The measured dN/dy at mid-rapidity for D^0 is $0.0265 \pm 0.0036(stat.) \pm 0.0071(syst.)$ and the measured D^{*+}/D^0 and D^+/D^0 ratios are approximately equal with a magnitude of $0.40 \pm 0.09(stat.) \pm 0.13(syst.)$. The total $c\bar{c}$ cross section per nucleon-nucleon collision extracted from this study is $1.18 \pm 0.21(stat.) \pm 0.39(syst.)$ mb. The direct measurement of open charm production is consistent with STAR single electron data. This cross section is higher than expectations from PYTHIA and other pQCD calculations. The measured p_T distribution is harder than the pQCD prediction using the Peterson fragmentation function.

PACS numbers: 25.75.Dw, 13.25.Ft, 14.40.Lb

1. Introduction

Study of open charm production provides valuable test of perturbative QCD (pQCD) predictions for heavy quark production [1]. There are significant uncertainties in the leading order (LO) and next-to-leading order (NLO) pQCD calculations of charm quark production depending on choices of the charm quark mass, the renormalization/factorization scale and the parton distribution function (PDF) [2]. Therefore, the open charm measurement provides a constraint on the parameters used in the pQCD calculations. The energy dependence of the $c\bar{c}$ production cross section is an important issue. Previously, most measurements of open charm production in hadronic interactions were from fixed-target experiments at lower energy ($\sqrt{s} \leq 63$ GeV). Only recently, CDF reported new results on open charm production in $p\bar{p}$ collisions in the high p_T region from the collider experiment at $\sqrt{s}=1.96$ TeV [3]. The open charm cross section has been studied in Au+Au collisions at $\sqrt{s_{NN}}=130$ GeV indirectly through measurements of single electrons from the open charm semi-leptonic decay [11].

The charm quark is generally believed to be produced primarily through gluon fusion ($gg \rightarrow c\bar{c}$) in parton-parton hard scattering due to its heavy mass, which makes

† atai@physics.ucla.edu, for complete author list, see Appendix of these proceedings.

the charm quark an important probe to the properties of matter formed in the early stage of relativistic heavy ion collisions. Theoretical calculations predicted that the open charm cross section in AA collisions would be significantly enhanced with respect to purely hadronic production [5] as a consequence of quark-gluon plasma (QGP) formation. Some studies have already attributed the increased yield of dileptons in the intermediate mass region reported by NA50 to open charm enhancement [6]. On the other hand, the open charm momentum spectrum may also be modified in AA collisions due to final state interactions such as parton energy loss in medium. However, it is predicted that energy loss of a charm quark should be considerably smaller compared to a light quark as a consequence of the dead-cone effect, leading to an enhanced D/π ratio as a function of p_T [7].

It is found that the relative fraction of the charm quark hadronization into different open charm species is nearly the same in elementary particle collisions (γp , e^+e^- , ep etc) [8]. Could the charm quark hadronization be modified in AA collisions? A calculation based on the Statistical Coalescence Model [18] does show that ratios of open charm species in AA collisions would be different from those in the elementary collisions. Furthermore, at RHIC, the predicted J/ψ suppression has to be investigated with respect to the total open charm cross section since the Drell-Yen cross section, which is the reference of the J/ψ suppression at SPS, is small in comparison with the open charm cross section at RHIC. In order to investigate the outstanding physics issues mentioned above, it is crucial to study open charm production in a less complicated system, where the nuclear effects, like QGP formation, parton energy loss, are not expected. The d +Au experiment at RHIC provides such an essential reference.

2. Data Analysis

The main detector involved in this data analysis is the STAR Time Projection Chamber (TPC) in a 0.5 T solenoidal magnetic field. A Zero Degree Calorimeter (ZDC) in the Au beam direction was used for the minimum bias trigger by requiring at least one beam-rapidity neutron in this ZDC. This trigger accepts $95\pm 3\%$ of the d +Au hadronic cross section. For a detail description of the STAR detector, see [10]. In this study, about 15 million d +Au minbias events with primary vertex position in beam direction within ± 75 cm around the TPC center were analyzed. The primary vertex reconstruction efficiency is $93\pm 1\%$ of triggered minimum bias events. The correlation between the measured momentum and the ionization energy loss (dE/dx) of charged particles in the TPC gas were used for particle identification. The measured $\langle dE/dx \rangle$ can be well described by the Bethe-Bloch function smeared with a resolution of width σ .

The open charm are reconstructed through their hadronic decay channels (and their charge conjugates): $D^0 \rightarrow K^-\pi^+$ (BR=3.8%), $D^0 \rightarrow K^-\pi^+\rho^0$ (BR = 6.2%) $\rightarrow K^-\pi^+\pi^+\pi^-$, $D^+ \rightarrow K^-\pi^+\pi^+$ (BR=9.1%) and $D^{*+} \rightarrow D^0\pi_s^+$ (BR = 68%) $\rightarrow K^-\pi^+\pi_s^+$. Event mixing technique [12] was used to reconstruct open charm mass peaks. The measured charged multiplicity distribution in the region of $|\eta| < 0.5$ was divided into

40 bins and the primary vertex position distribution was divided into 15 primary vertex bins. Each event was mixed with 5 other events within the same multiplicity bin and primary vertex bin. Tracks within 2σ of the pion Bethe-Bloch curve and 3σ of the kaon Bethe-Bloch curve were selected. In the momentum region of $p_T \gtrsim 0.6$ GeV/ c where the kaon and pion dE/dx bands merge, the nominal kaon and pion masses were assumed in turn for each track. It was also required that the closet approach distance of a track to the primary vertex, dca , be smaller than 1.5 cm with exception of the soft pions, π_s , from D^* decays where $dca < 3$ cm was used.

In the following subsections, We will discuss the analysis method for each decay channel.

2.1. $D^0 \rightarrow K^- \pi^+$ (+c.c.)

For this analysis only tracks within $|\eta| < 1$ were accepted. The transverse momentum and total momentum cut of a track were between 0.2 to 10 GeV/ c and 0.3 to 10 GeV/ c , respectively. The resulting invariant mass distribution after event-mixing background subtraction was shown in Fig.(1a), where a clear D^0 signal was seen alone with a residual background distribution. We fit the histogram with a Gaussian function for signal plus a linear background. From the fit, the mass and width (σ) of the D^0 signal was found to be 1.863 ± 0.003 GeV/ c^2 and 13.8 ± 2.8 MeV/ c^2 , respectively.

2.2. $D^0 \rightarrow K^- \pi^+ \rho^0$ (+c.c.)

An independent analysis for $D^0 \rightarrow K^- \pi^+ \rho^0$ was performed where only tracks within $|\eta| < 1.5$ were accepted. The transverse momentum and total momentum cut of a track were set between 0.3 to 10 GeV/ c . The analysis is similar to that for $D^0 \rightarrow K^- \pi^+$ except that additional π^+ and π^- candidate tracks, if their invariant mass satisfied 0.62 GeV/ $c < M(\pi^+ \pi^-) < 0.86$ GeV/ c , were combined with the selected K^- and π^+ candidate tracks to form a D^0 candidate with invariant mass $M(K^- \pi^+ \pi^+ \pi^-)$. The mass plot after event mixing background subtraction is shown in Fig.(1b). We fit the histogram with a Gaussian function for signal plus a linear background. From the fit, the mass and width (σ) of the D^0 signal were found to be 1.852 ± 0.005 GeV/ c^2 and 13.6 ± 4 MeV/ c^2 , respectively.

2.3. $D^{*+} \rightarrow D^0 \pi_s^+$ (+c.c.)

The track cuts for kaon and pion candidates from D^0 decay in the D^{*+} analysis were the same as those used in the $D^0 \rightarrow K^- \pi^+ \rho^0$ analysis. However, special treatments were needed for the soft pion daughter, π_s^+ , which has an average momentum of about 50 MeV. For the soft pion candidates it was required that the transverse momentum and total momentum cut be set between 0.1 to 1.0 GeV/ c and the ratio of the D^0 to π_s momentum, $p(D^0)/p(\pi_s) > 9.0$. First, the invariant mass of kaon and pion candidate tracks, $M(K\pi)$, was calculated and the D^0 candidate which satisfied $1.82 < M(K\pi) < 1.90$

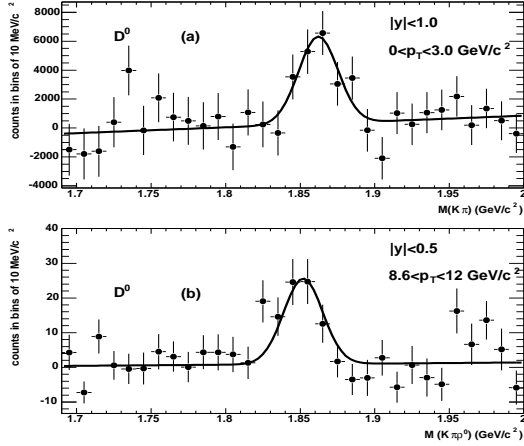


Figure 1. The D^0 signal reconstructed from $D^0 \rightarrow K^- \pi^+$ (+c.c.) (a) and the D^0 signal reconstructed from $D^0 \rightarrow K^- \pi^+ \rho^0$ (+c.c.) (b).

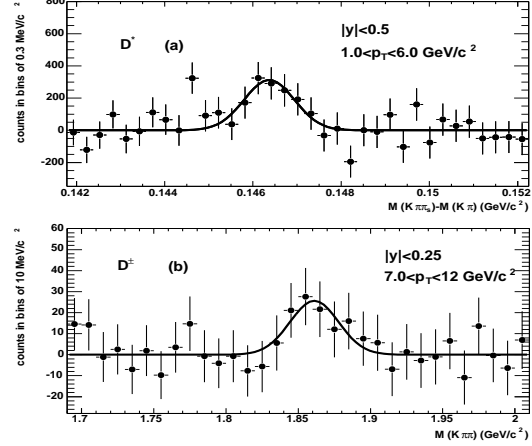


Figure 2. The D^* signal reconstructed from $D^* \rightarrow K^- \pi^+ \pi_s^+$ (+c.c.) (a) and the D^+ signal reconstructed from $D^+ \rightarrow K^- \pi^+ \pi^+$ (+c.c.) (b).

GeV/c^2 were kept. A soft pion candidate, with a charge opposite to that of the kaon candidate, was then combined with the D^0 candidate to form a D^* candidate with invariant mass $M(K\pi\pi_s)$. Fig.(2a) shows the distribution of the mass difference, $\Delta M = M(K\pi\pi_s) - M(K\pi)$, for $D^{*\pm}$ candidates after all cuts. A clear signal was seen around the nominal value of $M(D^{*\pm}) - M(D^0)$. We fit the mass distribution with a sum of a Gaussian function describing the signal and a linear background. From the fit, the mass difference and width (σ) of the D^{*+} signal were found to be $146.37 \pm 0.15 \text{ MeV}/c^2$ and $0.57 \pm 0.16 \text{ MeV}/c^2$.

2.4. $D^+ \rightarrow K^- \pi^+ \pi^+$ (+c.c)

The track cuts used for the D^\pm analysis were the same as those for the D^* analysis with the exception that no special treatment for the pion candidate was needed. Fig.(2b) shows the $M(K\pi\pi)$ distribution for the D^\pm candidates after all the cuts. A clear signal was seen at the nominal value of $M(D^\pm)$. The mass distribution was fit to a sum of a Gaussian function describing the signal and a linear background. From the fit, the mass and width (σ) of the D^{*+} signal were found to be $1.861 \pm 0.008 \text{ GeV}/c^2$ and $16.9 \pm 4.6 \text{ MeV}/c^2$.

3. Results and Discussions

Fig.(3) shows the invariant multiplicity distributions of the measured open charms as a function of p_T after the reconstruction efficiency correction, which is about 40%-60% (increasing with p_T) except for D^* at low p_T (eg. 6% at $p_T=1.5 \text{ GeV}/c$ due to the low

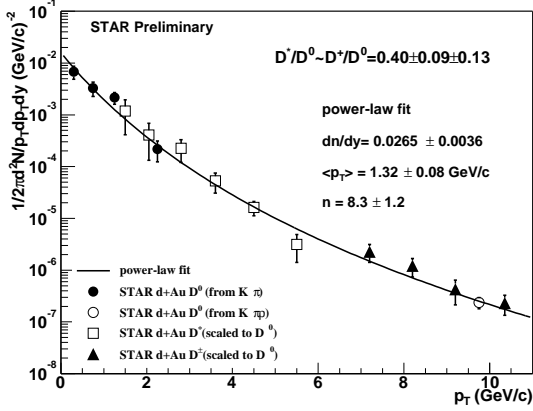


Figure 3. Measured invariant multiplicity distributions for D^0 , D^{*+} and D^+ and a power-law fit to the data points.

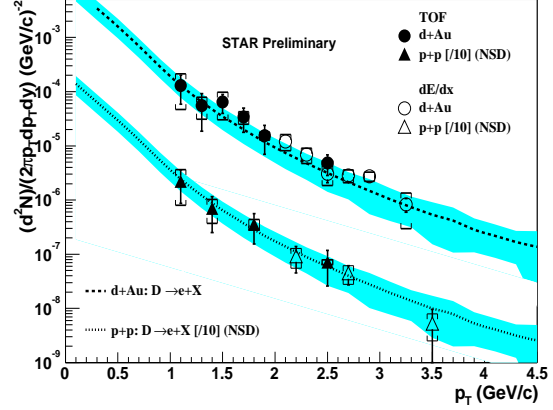


Figure 4. Consistency between directly measured open charm and the open charm measurements through single electrons.

reconstruction efficiency of the soft pions). The spectrum was corrected for vertex and trigger efficiency. For $D^0 \rightarrow K^+\pi^-$, a correction was also done through a Monte Carlo simulation for the correlation around the D^0 mass due to the misidentification of the kaon and pion from the D^0 decay. Errors of the data points are statistical only and the data have been divided by 2 assuming $\sigma(D) = \sigma(\bar{D})$. Overlap between D^0 and D^* at low p_T and between the D^0 and D^+ at high p_T allows us to compare the production cross sections of different open charm species. It was found that the inclusive cross sections of D^* and D^+ are approximately equal. This observation is consistent with the measurements in [3, 8].

With the ratio of $D^*/D^0 (=D^+/D^0)$ as a free parameter we fit the all data points by a power-law function, $A(1 + p_T/p_0)^{-n}$, where A , p_0 , and n are parameters. From the fit, we obtained: $dn/dy(D^0) = 0.0265 \pm 0.0036(stat.) \pm 0.0071(syst.)$ and $\langle p_T \rangle = 1.32 \pm 0.08(stat.) \pm 0.16(syst.)$ GeV/c. It was also found that $D^*/D^0 \approx D^+/D^0 = 0.40 \pm 0.09(stat) \pm 0.13(sys)$. The $c\bar{c}$ cross section can then be calculated by $\sigma_{c\bar{c}} = 1.24(\sigma_{D^0} + \sigma_{D^+})$, where the factor 1.24 includes the contribution from unmeasured D_s and charm baryons (Λ_c etc.) [8]. Assuming number of binary collision scaling, one could obtain σ_{D^0} for nucleon-nucleon collisions by $\sigma_{D^0} = 4.6 \times dn/dy(D^0) \times \sigma_{inel}/N_{bin}$, where $\sigma_{inel} = 42$ mb and $N_{bin} = 7.5$ [13] are the inelastic cross section for a nucleon-nucleon collision and number of binary collisions in $d+A$ collisions at $\sqrt{s_{NN}}=200$ GeV, respectively. The factor 4.6 accounts for the ratio of the D^0 multiplicity in the full rapidity region to $dn/dy(D^0)$ at mid-rapidity and was obtained from a PYHTIA [14] calculation with parameters tuned to fit our measured spectrum [15]. With the measured $dn/dy(D^0)$ and D^+/D^0 ratio, the $\sigma_{c\bar{c}}$ for nucleon-nucleon collisions is found to be $1.18 \pm 0.21(stat) \pm 0.39(sys)$ mb.

We also studied open charm production through measurements of single electrons from the open charm semileptonic decay. Fig.(4) shows the electron spectra for $d+Au$ and $p+p$ collisions at $\sqrt{s_{NN}}=200$ GeV, after background subtraction in comparison with the expected electron spectrum based on the decay of the STAR measured open charm spectrum (the bands). The background electrons are mainly from γ -conversion in the detector and from the π^0 and η Dalitz decay. The single electrons were measured by both Time of Flight (TOF) (solid symbols) and TPC dE/dx (open symbols). The width of the bands reflects the uncertainties in the calculation. For details about these measurements, see [16]. The open charm measurements through direct constructions of open charm signals and through the single electron measurement are consistent within STAR.

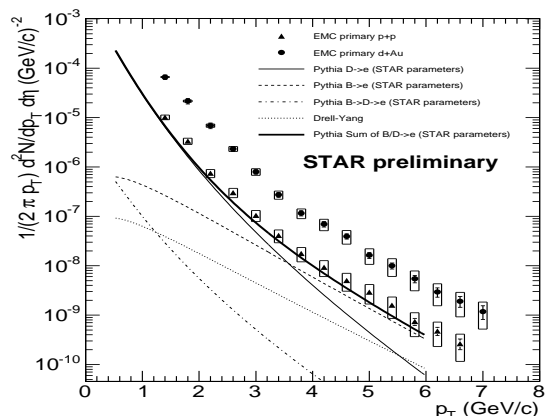


Figure 5. Background subtracted single electron spectra in $p+p$ and $d+Au$ collisions measured by STAR BEMC compared with a PYTHIA calculation.

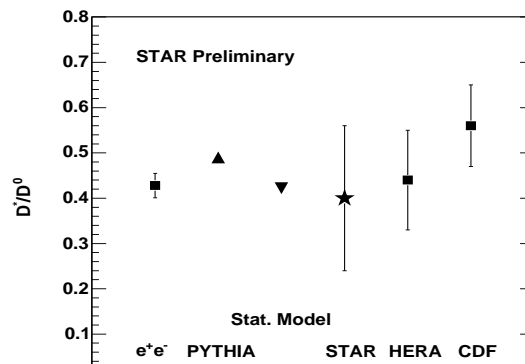


Figure 6. The STAR measured D^*/D^0 ratio in $d+Au$ collisions compared with other experimental data and with theoretical predictions.

The single electrons were also measured using the STAR Barrel Electromagnetic Calorimeter (EMC) up to 7.0 GeV/ c . Fig.(5) gives the background subtracted electron spectra for $d+Au$ (circles) and $p+p$ (triangles) collisions together with the calculations of PYTHIA with the modified parameters [15]. The PYTHIA curves shows that in the region of $p_T \gtrsim 4.0$ GeV/ c the contribution of B meson decays to electrons starts to overtake that of D meson decays, which is the clear indication at RHIC that the bottom quark contributes significantly to the measured high p_T electrons. For details of this analysis, see [17].

In Fig.(6), the STAR measured D^*/D^0 is compared with the previous measurements [3, 8] and with theoretical predictions [18]. Within the experimental uncertainties the ratio shows little dependence on collision system and energy.

The measured open charm spectrum is compared with theoretical predictions from

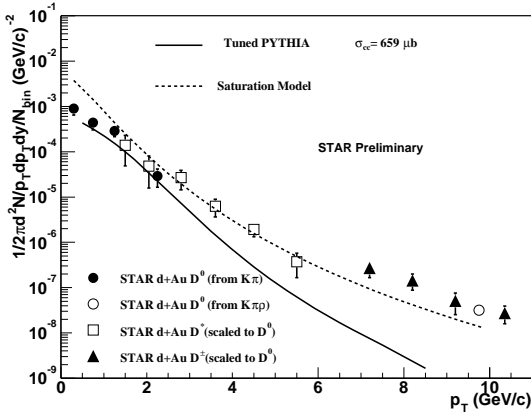


Figure 7. The measured open charm spectrum compared with PYTHIA and the Saturation Model.

the Saturation Model [19] and PYTHIA with parameters described in ref. [11] in Fig.(7). Note that the open charm spectrum has been scaled by $N_{bin} = 7.5$. One sees that the measured open charm spectrum is much harder than the PYTHIA prediction. However, the Saturation Model based on the k_T factorization scheme does predict a harder spectrum in comparison with one obtained from the LO pQCD calculation in PYTHIA.

In Fig.(8), the NLO pQCD predictions of the c-quark spectrum [20] are compared with the STAR open charm spectrum. The pQCD parameters in these calculations are m_c (charm quark mass)=1.2 GeV/ c^2 , μ_F (factorization scale)= μ_R (renormalization scale)=2 m_T (transverse mass of the charm quark) for the MRST HO PDF curve, and $m_c=1.3$ GeV/ c^2 , $\mu_F=\mu_R=m_T$ for the GRV98 HO PDF curve. The theoretical curves have been normalized to the measured cross section though the $c\bar{c}$ cross sections from NLO calculations significantly underestimates the measured one (eg. by a factor of 3 with the MRST HO PDF). It is interesting that the measured spectrum shape of the open charm coincides with those of the c-quark, especially the one obtained with GRV98 HO parton structure functions. Such a coincidence between the NLO c-quark spectrum and the measured open charm meson spectrum in charm hadroproduction has been observed in the fixed target experiments at low energies [21]. In order to fit with data, the intrinsic- k_T model had to be introduced to counter-balance the effect of c-quark hadronization through a fragmentation function of Peterson form [1, 21]. At RHIC, however, adding intrinsic- k_T with a moderate $\langle k_T^2 \rangle$ would not help to overcome the momentum degradation of the fragmentation process because the charm quark spectrum is very broad. Such an observation may indicate that the hadronization

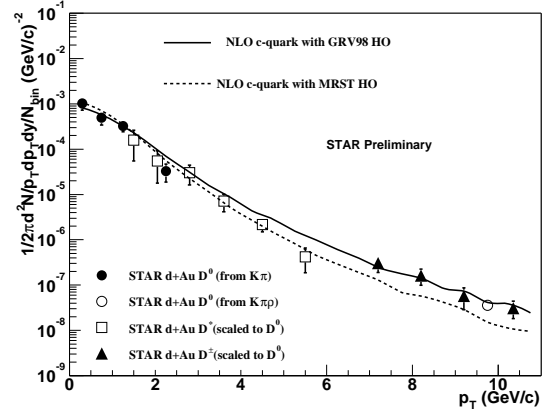


Figure 8. The measured open charm spectrum compared with NLO pQCD calculations for the charm quark. The theoretical curves have been normalized to the measured cross section.

of a c-quark through the Peterson fragmentation function, which was established in charm photoproduction [22] and in e^+e^- collisions [23], is not suitable in case of charm hadroproduction. Experimental data may suggest a fragmentation function more peaked towards the $x = 1$ region. A hadronization scheme of open charm production through quark recombination [24] was also proposed [25].

Acknowledgments

We wish to acknowledge the many helpful discussions with R. Vogt.

REFERENCES

1. Frixione S. *et al* 1997 *preprint* hep-ph/9702287
2. Vogt. R. 1996 *Z Phys. C* **71** 475
3. D. Acosta *et al* CDF Collaboration 2003 *Phys. Rev. Lett.* **91** 241894
4. Frixione S. *et al*) 1997 *Astrophys. Space Sci.* **10** 87
5. Shor A. 1988 *Phys. Lett. B* **215** 375; Shor A. 1989 *Phys. Lett. B* **233** 231; Shuryak E. 1992 *Phys. Rev. Lett.* **68** 3270.
6. Abreu M. C. *et al* 2000 *Eur. Phys. J.* **C14** 443
7. Kharzeev D. E. and Dokshitzer Y. L. 199 *Phys. Lett. B* **519** 199
8. Kniehl B. A. and Sefkow F. 2003 *preprint* hep-ph/0312054
9. Andronic A. *et al* 2003 *Nucl. Phys. A* **715** 529
10. Ackerman K. H. *et al* 2003 *Nucl. Instr. Meth.* **A499** 624
11. Adcox K. *et al* PHENIX Collaboration 2002 *Phys. Rev. Lett.* **88** 192303
12. L'Hote D. 1994 *Nucl. Instr. Meth. in Phys. Res.* **337** 544; Adler C. *et al* STAR Collaboration 2002 *Phys. Rev. C* **65** 041901(R)
13. Adams J. *et al* STAR Collaboration 2003 *Phys. Rev. Lett.* **91** 172302; Adams J. *et al* STAR Collaboration 2003 *Phys. Rev. Lett.* **91** 072304
14. Sjöstrand T. *et al* 2001 *Comput. Phys. Commun.* **135** 238
15. Modified PYTHIA parameters are: MSEL=1 (minbias events), CTEQ5M1 PDF, $\langle k_t \rangle = 2$ GeV/c, $m_c = 1.7$ GeV/c², $K_{factor} = 2.2$, MSTP(32)=4 (Q^2) and PARP(67)=4 (factor multiplied to Q^2).
16. Ruan L. J. for the STAR Collaboration these proceedings
17. Suaide A. for the STAR Collaboration these proceedings
18. Andronic A. *et al* 2003 *Phys. Lett.* **B571** 36 and private communication
19. Kharzeev D. and Tuchin K. 2003 *preprint* hep-ph/0310358
20. Vogt R. 2003 *Int. J. Mod. Phys.* **E12** 211 and private communication
21. Adamovich M. *et al* Beatrice Collaboration 1997 *Nucl. Phys.* **B495** 3
22. Gladilin L. for the ZEUS Collaboration 2003 *preprint* hep-ex/0309044
23. Nason P. and Oleari C. 2000 *Nucl. Phys.* **B565** 245
24. Hwa R. these proceedings
25. Rapp R. and Shuryak E. V. 2003 *Preprint* hep-ph/0301245